# ARTICLES

## Effect of Alcohols in AOT Reverse Micelles. A Heat Capacity and Light Scattering Study

**Silvia Perez-Casas,[†] Rolando Castillo,[‡] and Miguel Costas*[,†]**

*Laboratorio de Termofísica, Departamento de Física y Química Teórica, Facultad de Química, Universidad Nacional Autónoma de México, México D.F. 04510, México, and Instituto de Física, Universidad Nacional Autónoma de México, Apdo. Postal 20-364, México D.F. 01000, México*

*Received: January 7, 1997; In Final Form: June 17, 1997*[⊗]

Apparent molar heat capacities at 25 °C of a series of 1-alcohols and three branched alcohols were determined in mixtures of the type alcohol + (*p* wt % AOT + *n*-decane) at $R = 0$ and 10, $R$ being the water−surfactant molar ratio [W]/[S]. For methanol and 1-hexanol, the measurements were done for different $p$ values as a function of alcohol concentration. For all the other alcohols $p = 5$. Heat capacities for the binary (AOT + $nC_{10}$) and the ternary (AOT + W + $nC_{10}$) mixtures, as well as for 1-hexanol in a 5 wt % solution of dioctyl succinate, were also measured at 25 °C. For all alcohols + AOT + *n*-decane, kinematic viscosities and dynamic light scattering (DLS) were measured at 25 °C for $R = 10$ and $p = 13$ as a function of alcohol concentration. DLS was also measured for the ternary mixture AOT + W + $nC_{10}$ with $R = 10$ at 25 °C. A reasonable molecular picture of the alcohol−AOT interactions in the presence and absence of reverse micelles emerges from the experimental DLS and heat capacity results, the latter having been analyzed within the Treszczanowicz−Kehiaian model framework. In the absence of reverse micelles, all alcohols form complexes with the free AOT molecules in the solution, a process that competes with the alcohol self-association. The alcohol−AOT complex is most probably formed via an interaction between the hydroxyl group of the alcohol and the ionic head of AOT. When reverse micelles are present, two behaviors were found: (i) Methanol and ethanol are located in the micelle water pool; at low AOT concentration these alcohols only interact with water, but at higher AOT concentration they also form a complex with AOT molecules at the micellar interface. (ii) For butanol, longer 1-alcohols, and the three branched alcohols studied here two different processes occur: AOT molecules are withdrawn from the micelles to be complexed with alcohol molecules in the bulk of the solution, and alcohol molecules penetrate the micellar shell, where they also form a complex with AOT.

### I. Introduction

Reverse micelles are thermodynamically stable systems that are constituted by a surfactant, an organic solvent, and a small amount of water. These systems appear as homogeneous, transparent solutions that can solvate a wide range of hydrophilic compounds;[1] because of this property, reverse micelles are of interest in a variety of fields such as precipitation and crystallization, catalysis, semiconductor and magnetic particle formation, and stabilization of membrane mimetic systems where the surfactant assemblies are the host for the clustered particles.[2] The formation of reverse micelles requires the presence of water (W) which is solubilized in a polar core, forming the so-called water pool. These structures are then spherical droplets of water dispersed in oil. Their spontaneous curvature arises from the energetically favorable packing configuration of the surfactant molecules at the water−oil interface and depends basically on the molecular geometry of the surfactant molecule;[3] therefore, to understand the behavior of reverse micelles, geometrical models have been very helpful.[4] The radius of the water pool, and hence the size of the reverse micelle, is mainly characterized by $R = [H_2O]/[S]$, the water−surfactant molar ratio. When small amounts of water are present ($R \leq 15$), the aggregates formed in solution are called reverse micelles, whereas the dispersions formed when larger quantities of water are present ($R \geq 15$) are termed microemulsions; these dispersions contain both droplets and random bicontinuos structures.

One of the surfactants often used to form reverse micelles and microemulsions is sodium bis(2-ethylhexyl)sulfosuccinate (sulfobutanedioic acid 1,4-bis(2-ethylhexyl) ester sodium salt), usually called Aerosol OT or AOT. Experimental studies using this anionic surfactant have employed a variety of spectroscopic techniques such as photon correlation[5] and small angle neutron[6] and X-ray[7] scattering. Thermodynamic studies aimed at the determination of apparent molar volumes, heat capacities, and enthalpies have also provided valuable physical insights.[8] A comprehensive picture of the behavior of AOT−W−oil mixtures has been reached as a result of all those studies, which have used a range of $R$ values covering both the reverse micelle and the microemulsion cases and several solvents (isooctane, cyclohexane, *n*-decane, etc.). In contrast, an area much less explored is that of the study of the interaction of reversed micelles with a fourth component which, in the case of microemulsions, is usually called cosurfactant. It is in this area where the objectives of the present work are placed. We have studied the effect over AOT reverse micelles ($R = 10$, with *n*-decane as the oil or solvent) of a series of linear and some branched alcohols as a function of AOT and alcohol concentra-

* To whom correspondence should be addressed. E-mail: miguel@mizton.pquim.unam.mx.
[†] Laboratorio de Termofísica.
[‡] Instituto de Física.
[⊗] Abstract published in *Advance ACS Abstracts,* August 1, 1997.

S1089-5647(97)00108-9 CCC: $14.00 

tion. The effect of linear alcohols on AOT−W−oil systems has been studied before for the case of reverse micelles using IR spectroscopy[9] and employing small angle neutron[10] and light[11] scattering for the microemulsion case ($R = 20$ and 30, respectively); the main results from these studies will be commented on below and, when possible, compared against those presented here. In this work, we have employed heat capacity measurements that are particularly sensitive to the formation or destruction of organization or structure in the bulk of liquid mixtures.[12] For comparison with the $R = 10$ case, mixtures with $R = 0$, *i.e.*, those where water and hence reverse micelles are not present, have also been studied. For the $R = 10$ case, dynamic light scattering (DLS) experiments were performed to determine the *z*-averaged translational diffusion coefficient and the corresponding hydrodynamic radius of the reverse micelles systems with and without alcohol. The Treszczanowicz−Kehiaian (TK) model[13,14] has been used here as the theoretical framework to interpret our heat capacity data; this association model has proven to be a useful tool to understand the self-association of an alcohol in an inert (*n*-alkane) solvent, as well as the formation of complexes between alcohol and proton acceptor molecules[15,16] such as AOT. A review of the TK model is presented in section II, the experimental details and procedures are described in section III, and the heat capacity and DLS results are discussed in detail in section IV.

## II. The Treszczanowicz−Kehiaian Association Model

The original TK model[17] was developed to study association (self and cross association) in liquid mixtures, the most common case being that where the association occurs via the formation of H-bonds. It has several basic assumptions, namely, (i) it is considered that the enthalpy of mixing arises only from the formation of species in solution, *i.e.*, it is an "athermal model"; as such, the TK model deals only with the so-called chemical contributions to the thermodynamic properties, the physical contributions being all those arising from interactions in the system other than the association itself, (ii) the enthalpy of association corresponding to the addition of a monomer to a given self-associated species $\Delta H_{i,i+1}$ and that corresponding to the formation of cross association $\Delta H_{i,j}$ are independent of *i* and *j*, and (iii) there are no volume changes due to the association, *i.e.*, the excess volume is assumed to be zero. The original TK model has been extended a number of times[13,15] in order to study different kinds of associated mixtures. In particular, the extension to the case of ternary mixtures[13,14] of the type A + (B + I) is relevant for the present work; here, A is a liquid capable of self-association such as an alcohol (component 1), B (component 2) is a compound, usually a proton acceptor such as AOT, which is unable to self-associate but can associate with A to form complexes or cross species, and I is an inert solvent (component 3) such as *n*-decane ($nC_{10}$). When $R = 10$, *i.e.*, when water is present, component B will be taken as a pseudocomponent formed by AOT and W; some authors[8b] refer to this pseudocomponent as the "micellar matter".

The relevant thermodynamic quantity is the associational part of the apparent molar heat capacity of the alcohol, which is experimentally obtained from

$$\phi_c(\text{assoc}) = \phi_c - \lim \phi_c^b(x_1 \rightarrow 0) \qquad (1)$$

where $\phi_c$ is the measured apparent molar heat capacity of the alcohol in the mixture (A + B + I) and $\lim \phi_c^b(x_1 \rightarrow 0)$ is the infinite-dilution value (obtained by extrapolation to zero alcohol concentration) of the alcohol apparent heat capacity in the alcohol + inert solvent (A + I) binary mixture. This infinite-dilution limit represents the contribution to the heat capacity of the alcohol in the absence of any association, *i.e.*, the so-called physical contributions which are assumed to be independent of alcohol concentration. $\phi_c$(assoc) is given explicitly by the TK model as[13]

$$\phi_c(\text{assoc}) = \left\{\left(\frac{\Delta H^\circ}{T}\right)^2 \frac{1}{R}\left\{\sum_{i=2} \frac{i-1}{i} K_i^\varphi \frac{\phi_A^i}{\phi_1}[(i-1)]\left(\frac{\phi_2 X}{r} + 1\right) + \sum_{j \neq i} (i-j) K_j^\varphi \phi_A^{j-1}\right\} + \frac{\Delta H^\circ \, \Delta H_{11}^\circ}{RT^2}\left(\frac{2\phi_2 X}{r\phi_1} \sum_{i=2} (i-1) K_i^\varphi \phi_A^i\right) + \left(\frac{\Delta H_{11}^\circ}{T}\right)^2 \frac{1}{R}\left[\frac{\phi_2 X}{r\phi_1}(\phi_A + \sum_{i=2} i K_i^\varphi \phi_A^i)\right]\right\} \Bigg/ \left(1 + \sum_{j=2} j K_j^\varphi \phi_A^{j-1} + \frac{\phi_2 X}{r}\right) \qquad (2)$$

where

$$X = \frac{[r/(r+1)]K_{11}^\varphi}{([r/(r+1)]K_{11}^\varphi \varphi_A + 1)^2} \quad \text{and}$$

$$\phi_1 = \frac{x_1}{x_1 + r x_2 + r_1 x_3} \qquad (3)$$

In eq 2, the only cross associated species considered is the 1:1 complex $A_1B_1 = AB$, which is characterized by the volumetric equilibrium constant $K_{11}^\varphi$ and by the enthalpy change for the formation of this species $\Delta H_{11}^\circ$, $\phi_1$ is the alcohol volume fraction in solution, $\Delta H^\circ$ represents the alcohol self-association enthalpy change corresponding to the formation of 1 mol of H-bonds, $K_i^\varphi$ are the volumetric equilibrium constants for each $A_i$ species in solution, and $\phi_A$ is the volume fraction of the alcohol in solution that is in the form of monomers. This fraction is obtained as the closest root to zero of the mass balance equation

$$\sum_{j=2} K_j^\varphi \phi_A^j + \phi_A - \phi_1 + \frac{\phi_2}{r}\left(\frac{[r/(r+1)]K_{11}^\varphi \phi_A}{[r/(r+1)]K_{11}^\varphi \phi_A + 1}\right) = 0 \qquad (4)$$

which can be easily found using the Newton−Raphson numerical method.[18] In eqs 2−4, $r_1$ is the ratio of molar volumes $V_3/V_1$ and $r = V_2/V_1$ when component 2 is AOT ($R = 0$) or $r = V_2'/V_1$ when component 2 is the pseudocomponent AOT + W ($R = 10$); in this case, $V_2' = x_{AOT}V_{AOT} + x_W V_W$ with $x_{AOT} + x_W = 1$.

It is also important to examine the infinite-dilution limit of the associational part of the apparent molar heat capacity of the alcohol in the ternary mixture, *i.e.*, $\lim \phi_c(\text{assoc})(x_1 \rightarrow 0)$, which corresponds to the situation where an alcohol molecule is unable to self-associate with other alcohol molecules, but it is able to form a complex with the proton acceptor molecules of compound B. This limit can be experimentally obtained from eq 1 as

$$\lim \phi_c(\text{assoc})(x_1 \rightarrow 0) = \lim \phi_c(x_1 \rightarrow 0) - \lim \phi_c^b(x_1 \rightarrow 0) \qquad (5)$$

and from the TK model, using eqs 2−4, as

$$\lim \phi_c(\text{assoc})(x_1 \rightarrow 0) = \left(\frac{\Delta H_{11}}{T}\right)^2 \frac{1}{R} \frac{K_{11}^{\varphi} \Omega_2^*/(1+r)}{[1+(K_{11}^{\varphi}\Omega_2^*)/(1+r)]^2} \quad (6)$$

where $\Omega_2^* = x_B/(x_B + (V_B/V_C)x_C)$, with $x_B + x_C = 1$, $V_B = V_2$ for $R = 0$ and $V_B = V_2'$ for $R = 10$, and $V_C = V_3 = V_{nC_{10}}$; as such, $\Omega_2^*$ is the volume fraction of B in the mixture B + I. In accordance with the experimental results from eq 5 (see section IV), eq 6 predicts that a plot of lim $\phi_c$(assoc)($x_1 \rightarrow 0$) against $\Omega_2^*$ must display a maximum occurring at

$$\Omega_2^*(\max) = (1+r)/K_{11}^{\varphi} \quad \text{and} \quad \lim \phi_c(\text{assoc})(\max) = \Delta H_{11}^2/4RT^2 \quad (7)$$

Equation 7 can then be used to evaluate from the experimental $\Omega_2^*$(max) and lim $\phi_c$(assoc)(max) values the $\Delta H_{11}$ and $K_{11}^{\varphi}$ for the alcohol−AOT association or complex formation. In practice, however, it is more convenient to obtain the $\Delta H_{11}$ and $K_{11}^{\varphi}$ parameters from a fit of eq 6 to the experimental results.

## III. Experimental Section

Apparent molar heat capacities $\phi_c$ at 25 °C of a series of 1-alcohols ($C_mH_{2m+1}OH$ with $m$ = 1, 2, 3, 4, 6, 8, 12, and 16) and 2-methylcyclohexanol (mixed isomers), 3-ethyl-3-pentanol, and cholesterol were determined in mixtures of the type alcohol + ($p$ wt % AOT + $n$$C_{10}$) with $R = 0$ and 10; here, $p$ denotes the weight percent of AOT in the binary (AOT + $n$$C_{10}$), for both $R = 0$ and 10. For methanol and 1-hexanol, the measurements were done for different $p$ values as a function of alcohol concentration (from extreme dilution up to 5 wt %, except for those cases where the solubility of the alcohol is lower). For all the other alcohols $p = 5$. Heat capacities for the binary (AOT + $n$$C_{10}$) and the ternary (AOT + W + $n$$C_{10}$) mixtures were also measured as a function of AOT concentration, at 25 °C. In addition, the apparent molar heat capacities of 1-hexanol in a 5 wt % solution of butanedioic acid 1,4-bis-(2-ethylhexyl) ester (dioctyl succinate or DOS) + $n$$C_{10}$ were determined as a function of alcohol concentration at 25 °C. For all alcohols, kinematic viscosities and DLS were measured at 25 °C for $R = 10$ and $p = 13$, as a function of alcohol concentration. DLS was also measured for the ternary mixture AOT + W + $n$$C_{10}$ with $R = 10$ at 25 °C. For all the mixtures discussed in this work, heat capacity, kinematic viscosity, and diffusion coefficients data can be found as Supporting Information.

**Materials.** All materials were from Aldrich Chemical Co. with a stated purity of at least of 99%. Water was doubly distilled. AOT ($C_{20}H_{37}NaO_7S$) was stored on $P_2O_5$ in a desiccator. Its water content was determined periodically using the Karl Fisher titration method; an average of 1.5 wt % of water ($R = 0.38$) was found over a two-year period. In order to avoid the slow hydrolysis of AOT + W + $n$$C_{10}$ solutions,[19] all the measurements were done with freshly prepared samples. Alcohols were stored over molecular sieves.

**Procedure.** *Sample Preparation.* Samples were prepared by weight (Mettler AT-250). To obtain the desired $R = 10$ value, water was added to a AOT + $n$$C_{10}$ binary solution of known concentration; different amounts of alcohol were then added to this stock ternary solution to obtain the samples for the heat capacity, density, viscosity, and DLS measurements. For the $R = 0$ case, known amounts of alcohol were added to an AOT + $n$$C_{10}$ binary mixture. The lowest $R$ values for which AOT reverse micelles have been detected are (i) 0.7 ± 0.2, using small angle neutron scattering and $n$$C_{10}$ as solvent,[7] and (ii) between 4.0 and 5.0 using heat capacity measurements in cyclohexane.[8a] Hence, the AOT water content reported above is not enough to form reverse micelles, and we can consider that in our $R = 0$ samples (strictly, $R = 0.38$) AOT is free or randomly dispersed in the solution. On the other hand, since the reported[6] critical micelle concentration (cmc) for AOT in $n$$C_{10}$ (0.045 wt % at $R = 30$ by X-ray scattering) is much lower than the smallest AOT concentration used here ($p = 0.27$ wt % for the case of AOT + W + $n$$C_{10}$ and $p = 0.21$ wt % when an alcohol was added), all our measurements with $R = 10$ are in the concentration region where reversed micelles are present. The estimated uncertainty in the quoted concentrations (wt %) is less than 0.02. The ternary reverse micelles mixtures (AOT + W + $n$$C_{10}$) used in this work are located in the oil-rich region of the phase diagram,[20] as indicated in Figure 1.

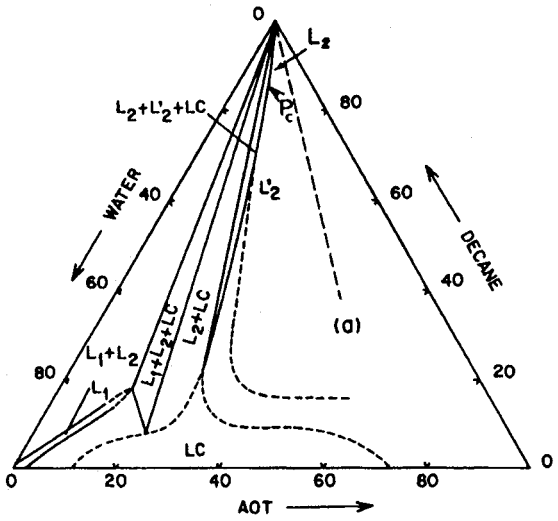


**Figure 1.** Phase diagram for AOT + W + $n$$C_{10}$ taken from ref 20. The slashed line (a) in the oil-rich region indicates the $R = 10$ water−AOT molar ratio.

*Determination of the Heat Capacities and Calculation of $\phi_c$.* Volumetric heat capacities were measured using a Picker flow microcalorimeter (Sodev Inc., Canada) with the procedures described in the literature.[21] The volumetric heat capacities were converted into molar heat capacities using densities obtained with a vibrating-cell densimeter (Sodev Inc., Canada). For very dilute alcohol concentration, the heat capacity of the solutions was determined using $n$$C_{10}$ as the reference liquid ($C^{\circ}_{p,nC_{10}}$ = 314.42 J $K^{-1}$ $mol^{-1}$ from ref 22); for more concentrated solutions, the previous less concentrated solution was employed as reference. The reproducibility of the $\phi_c$ results under nominally identical experimental conditions was better than 10 J $K^{-1}$ $mol^{-1}$; this represents between 1.5 and 4% of the $\phi_c$ value, depending on the system.

The measured heat capacity data allow the calculation of several different apparent molar heat capacities $\phi_c$. For instance, for the quaternary solutions alcohol + (AOT + W + $n$$C_{10}$), it is possible to calculate $\phi_c$ for the alcohol or $\phi_c$ for the assembly [alcohol−AOT−W] or $\phi_c$ for the assembly [AOT−W], or for other assemblies. In general, the expression to calculate the apparent molar heat capacity of a single component or assembly α is

$$\phi_{c,\alpha} = (C_p^{\text{sol}} - x_\beta C_{p,\beta})/x_\alpha \quad (8)$$

where $C_p^{\text{sol}}$ is the measured heat capacity and $x_\alpha + x_\beta = 1$. Depending on the choice for α, $x_\alpha$, $x_\beta$, and $C_{p,\beta}$ represent different quantities. The cases of interest in this work are as

follows: (i) for the binary mixtures AOT + $n$C$_{10}$, α = AOT and hence $\beta = n$C$_{10}$, (ii) for the ternary mixtures AOT + W + $n$C$_{10}$, α = AOT−W and hence $\beta = n$C$_{10}$, (iii) for the ternary mixtures alcohol + AOT + $n$C$_{10}$, α = alcohol and hence $\beta$ = AOT−$n$C$_{10}$, and (iv) for the quaternary mixtures alcohol + AOT + W + $n$C$_{10}$, α = alcohol and hence $\beta$ = AOT−W−$n$C$_{10}$. For cases (iii) and (iv), $C_{p,\beta}$ was measured using $n$C$_{10}$ as the reference liquid.

It is important to note that studying AOT reverse micelles systems, some authors[8] have elected to study the behavior of the apparent molar heat capacity of the micellar matter MM, *i.e.*, of the assembly AOT−W, given by

$$\phi_c^{MM} = Mc + \frac{1000(c - c_0)}{m} \tag{9}$$

where $c$ and $c_0$ are the specific heat capacities (J K$^{-1}$ g$^{-1}$) of the solution and the solvent, respectively, $m$ is the molality of AOT in $n$C$_{10}$, and $M$ the molar mass of the micellar matter calculated as $M = M_{AOT} + RM_W$. When an alcohol is added, *i.e.*, for the quaternary mixtures studied here, eq 9 can also be used with $M = M_{AOT} + RM_W + R'M_{OH}$, where $M_{OH}$ is the molar mass of the alcohol and $R' = [OH]/[AOT]$ is the alcohol−AOT molar ratio. Through algebraic manipulation of eq 8 and 9, it can be shown that $\phi_{c,\alpha} = \phi_c^{MM}/(1 + R)$ and $\phi_{c,\alpha} = \phi_c^{MM}/(1 + R + R')$ with α = AOT−W for the ternary and quaternary solutions, respectively. It appears then that the quantities $\phi_{c,\alpha}$ and $\phi_c^{MM}$ are proportional to each other, and either eq 8 or 9 can be used to study the behavior of the micelar matter in the presence and absence of alcohol molecules.

*Determination of Kinematic Viscosities.* Dynamic viscosities of the same samples used for the DLS measurements were determined at 25 °C with a Canon Fenske viscometer. These dynamic viscosities were converted into kinematic viscosities through density data obtained as described above.

*Dynamic Light Scattering Measurements.* DLS was used to determine the *z*-averaged translational diffusion coefficient and the corresponding hydrodynamic radius of the reversed micelles. In our experimental configuration, laser light is produced by an argon-ion laser (Spectra Physics 2060-4S, Mountain View, CA), operating at a wavelength of 514.5 nm. The laser beam is focused in the center of a round cuvette containing the sample, at 30° from the detection direction. Cuvettes, scrupulously cleaned, containing a few milliliters of doubly filtered (0.22 μm filters, Millipore) freshly prepared solutions are immersed in a temperature controller circular water bath, placed in the scattering area. The temperature is kept constant at 25 ± 0.1 °C, with the aid of a controller (Tronac PTC-41, Canada). Temperature measurements are done with a resistance thermometer (Cole-Parmer 8502-16). The solid angle subtended by the scattering volume and the photomultiplier is optimized for dynamic light scattering by mounting two 600-μm pinholes in the optical detection system. Dispersed light is detected with a photomultipler (THORN EMI 9863/100, England), and electrical signals are preamplified and shaped with a preamplifier/discriminator (ALV/PM-PD, Germany). Counts per second and correlation functions were obtained by a multiple-tau digital correlator (ALV-5000, Germany). Light scattering measurements were obtained after at least 20 min of thermal stabilization for the samples. Typical scattering times were 10 min at about ∼75 mW incident power. DLS measures the intensity fluctuations that occur over short time intervals due to the Brownian motion of the micelles in solution. The time behavior of these fluctuations is described quantitatively by the intensity autocorrelation function. The measured normalized intensity autocorrelation function, $g_2(q,t)$, was related to the normalized field autocorrelation function $g_1(q,t)$ using the Siegert relation,[23] $g_2(q,t) = 1 + B[g_1(q,t)]^2$. Here, $q = 4\pi\eta/\lambda_0 \sin(\theta/2)$ is the wave vector in the scattering event, $n$ is the refractive index, $\lambda_0$ is the incident wavelength in vacuum, $\theta$ is the scattering angle, and $B$ is a characteristic of the optical detection system. The time constants were obtained fitting the correlation functions, using the method of cumulants developed by Koppel.[24]

In the high-dilution limit, the diffusion coefficient of spherical particles suspended in a solvent can be related to their radius $r$ through the Stokes−Einstein relation $D = k_bT/(6\pi\eta r)$; here, $k_b$ is the Boltzmann constant, $T$ is the absolute temperature, and $\eta$ is the viscosity of the solvent. We tested our DLS equipment and technique with certified polystyrene microspheres of 96 ± 3 nm diameter (Duke Scientific Co., CA) in aqueous solution. We obtained the diffusion coefficient ($q = 2.3 \times 10^7$ m$^{-1}$) at infinite dilution and, through the Stoke−Einstein relation, the radius of the microspheres, which was within the certified uncertainty. We also tested our procedure measuring reverse micelles in microemulsions formed by AOT + W + $n$C$_{10}$ at $R$ = 41.2 and 25 °C, where Dozier *et al*. have reported light scattering measurements.[5b] In this case, the diffusion coefficient $D$ is given by

$$D(\phi') = D_0(1 + k_1\phi' + k_2\phi' + ...) \tag{10}$$

where $k_i$ are constants and the volume fraction $\phi' = 1 - (V_s/V_m)$, with $V_s$ being the volume of the solvent added to make a total volume $V_m$ of microemulsion. We measured $D(\phi')$ and obtained a $D_0$ limiting value; from these data, we obtained a hydrodynamic radius of the reverse micelles that agreed, within the experimental error, with that reported in ref 5b.

## IV. Results and Discussion

**AOT + Water + *n*-Decane Systems ($R = 0$ and $R = 10$).** *Dynamic Light Scattering.* Using the procedures described above, DLS was determined for AOT + W + $n$C$_{10}$ with $R$ = 10. Employing eq 10, we obtained $D_0 = 4.61 \times 10^{-11}$ m$^2$ s$^{-1}$ ($q = 9.23 \times 10^6$ m$^{-1}$) and $k_1 = -28.8$, giving a hydrodynamic radius for the reverse micelles of $5.5 \times 10^{-9}$ m. This radius is bigger than that obtained extrapolating Dozier *et al*'s values at $R$ = 24.7, 32.9, and 41.2.[5b] Due to the small water pool of the micelles at $R = 10$, density fluctuations caused by the Brownian motion of the micelles are difficult to detect with DLS, particularly at high dilution; therefore, the limiting $D_0$ value at $R = 10$ cannot be as precise as for larger $R$ values. On the other hand, the observed discrepancy between the measured and extrapolated hydrodynamic radius values is consistent with the fact that the $R = 10$ value we used here is within a small region of $R$ values where abnormalities in the behavior of some properties have been observed by several workers using different techniques; for example, (i) Eicke *et al*.[25] found that between $R$ = 6 and 12 the mean apparent molecular weights and the proton NMR chemical shifts for AOT + W + isooctane show a clear change of slope; these results were interpreted in terms of the possible existence of a so-called "transition" region between a micellar state (where swelling is observed) and a microemulsion domain with larger reverse micelles, and (ii) Tanaka *et al*.[26] found that the measured dielectric constant for AOT + W + cyclohexane mixtures showed a maximum at $R$ = 5 and a minimum at $R = 15$; this abnormal dielectric response has been attributed to a change in the polarity of the water pool, revealing two differently structured reverse micelles. Our own preliminary DLS results with AOT + W + $n$C$_{10}$ (not reported here) show that the behavior of $D_0$ as a function of $R$ is also abnormal: the linear increase of $D_0$ when $R$ decreases found at

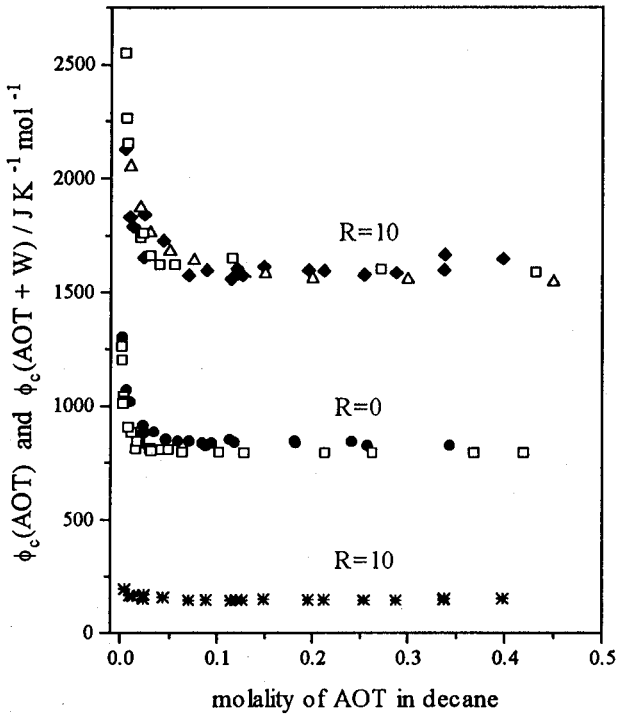


**Figure 2.** Apparent molar heat capacities (●) at 25 °C for free AOT in the mixture AOT + $n$C$_{10}$ ($R$ = 0) and for the assembly or micellar matter AOT−W in AOT + W + $n$C$_{10}$ ($R$ = 10) using eq 8 (*) and eq 9 (◆). For $R$ = 0, both equations give the same result. For $R$ = 10, both curves are related as described in the text. For comparison, data for AOT + W + $n$C$_{10}$ (△) from ref 8b and for AOT + cyclohexane and AOT + W + cyclohexane (□) from ref 8a are also shown.

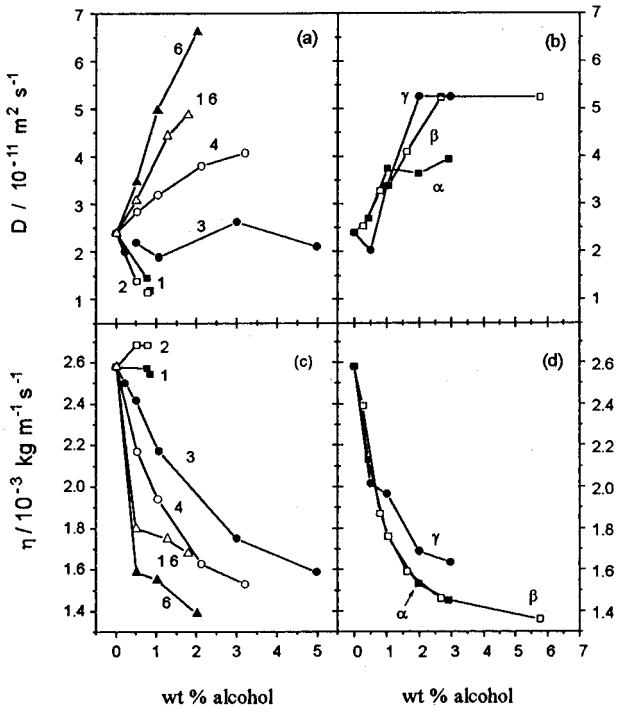


**Figure 3.** Diffusion coefficients $D$ (a and b) and kinematic viscosities $\eta$ (c and d) for linear and branched alcohols at 25 °C as a function of alcohol concentration for the quaternary mixtures alcohol + (13 wt % AOT + $n$C$_{10}$) with $R$ = 10. Numbers in a and c represent the alcohol carbon number. Branched alcohols in b and d are 2-methylcyclohexanol (mixed isomers) (α), 3-ethyl-3-pentanol ($\beta$), and cholesterol ($\gamma$). Lines are only to aid visualization.

large $R$ values changes at $R \cong 20$, where $D_0$ starts to decrease, to reach a minimum at $R \cong 14-18$ and then to increase again for smaller $R$ values (with a steeper slope than that observed at high $R$ values). The verification of these results is certainly important, and hence work in this direction is currently under way.

*Apparent Heat Capacities.* The apparent molar heat capacities for free AOT in the mixture AOT + $n$C$_{10}$ ($R$ = 0) and for the assembly AOT−W in AOT + W + $n$C$_{10}$ ($R$ = 10) obtained using eqs 8 and 9 are shown in Figure 2; for the $R$ = 0 case, MM in eq 9 is only AOT, in hence eqs 8 and 9 give the same result. For comparison, similar data from ref 8b in $n$C$_{10}$ and from ref 8a in cyclohexane are also displayed. The agreement between the data reported here and that from ref 8b for $R$ = 10 is excellent. Figure 2 also shows that in this concentration region the behavior of both free AOT and reverse micelles is the same in both inert solvents. Note that the characteristic peak in $\phi_c$ found for other surfactants at their cmc[27] appears in the present $R$ = 10 system at an AOT concentration which is much lower (AOT molality of 0.001) than those displayed in Figure 2 (see ref 8a). As seen in Figure 2, adding water to the AOT + $n$C$_{10}$ system displaces the $R$ = 0 curve in different directions depending on the way the apparent molar heat capacity of the assembly AOT−W or micellar matter is calculated; that is if eq 8 is employed, the curve is moved toward lower values, while if eq 9 is used, it is moved to higher values; both $R$ = 10 curves are related, as shown above, by $\phi_{c,\alpha} = \phi_c^{MM}/(1 + R)$. This behavior follows from the different definitions of the solute that are employed in eqs 8 and 9, namely, an AOT molecule + $R$ water molecules for eq 9 and an "average solute molecule" constituted by one AOT molecule and $R$ water molecules for eq 8. Both definitions of the solute are meaningful, but for the micellar matter case, eq 9 has a more clear physical significance. This is clearly seen considering that the difference between the $R$ = 10 and $R$ = 0 curves at $m > 0.1$ mol Kg$^{-1}$ is an average value of 764 J K$^{-1}$ mol$^{-1}$, which is very close to 750 J K$^{-1}$, the heat capacity of 10 mol of water; if the same simple calculation is done for the data at $R$ = 20 in ref 8b, the result is 1522 J K$^{-1}$ mol$^{-1}$, which again is very close to 1500 J K$^{-1}$, the heat capacity of 20 mol of water. These observations have been done before[8] and clearly support the physical image of water being incorporated in the hydrophilic micellar core. They also imply that the properties of water in the reverse micelle core are close to those of bulk water. This is surprising given that the maximum amount of water bound to AOT corresponds[25,28] to a $R$ value of about 10; that is nearly all of the water molecules at $R$ = 10 are hydration water.

**Alcohol + AOT + Water + *n*-Decane Systems ($R$ = 0 and $R$ = 10).** *Dynamic Light Scattering and Kinematic Viscosities.* The measured diffusion coefficients $D$ and kinematic viscosities $\eta$ at 25 °C as a function of alcohol concentration for the quaternary mixtures alcohol + ($p$ wt % AOT + $n$C$_{10}$) with $R$ = 10 and $p$ = 13 are shown in Figure 3. At zero alcohol concentration $D = 2.28 \times 10^{-11}$ m$^2$ s$^{-1}$ ($q = 9.51 \times 10^6$ m$^{-1}$). For methanol, ethanol, hexanol, and hexadecanol measurements were done up to an alcohol concentration that is very close to their solubility in AOT + W + $n$C$_{10}$. Figure 3 indicates that there is a pronounced effect on the diffusion coefficient for the micelles when different alcohols are added: $D$ decreases for the shortest chain alcohols methanol and ethanol, remains practically without change for propanol, and increases for butanol, the longer alcohols, and the branched alcohols. Note that at low alcohol concentrations, the slope of $D$ with alcohol concentration is very similar, but of opposite sign, for 1-hexadecanol and the three branched alcohols, and either methanol or ethanol. Figure 3 also shows that the addition of methanol or ethanol does not change the kinematic viscosity, whereas

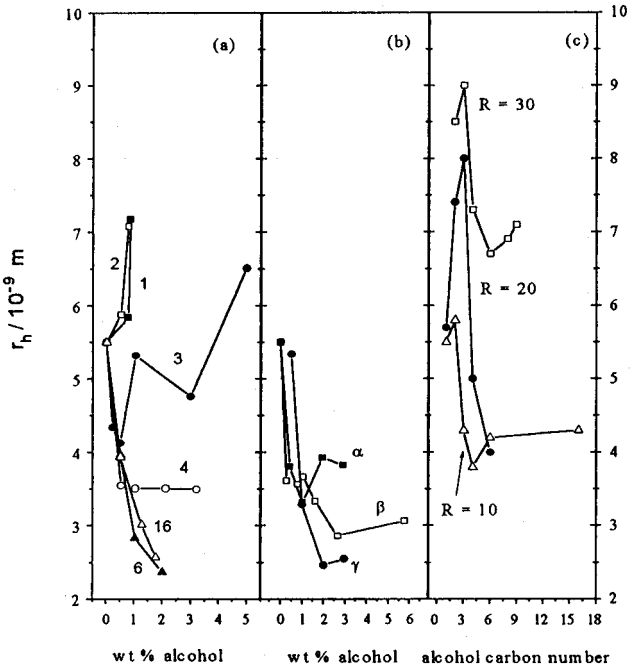


**Figure 4.** Hydrodynamic radius $r_h$ of the reverse micelles in the presence of linear alcohols (a) and branched alcohols (b). Numbers in a represent the alcohol carbon number. Branched alcohols in b are 2-methylcyclohexanol (mixed isomers) (α), 3-ethyl-3-pentanol ($\beta$), and cholesterol ($\gamma$). The behavior of $r_h$ with alcohol carbon number and $R$, at constant alcohol concentration, is shown in c. Data for $R = 10$ are from this work, for $R = 20$ from ref 10, and for $R = 30$ from ref 11. For $R = 10$ and 30, the alcohol concentration is 0.4 wt %; for $R = 20$, the alcohol concentrations are (wt %) 0.46 for methanol, 0.65 for ethanol, 0.84 for propanol, 1.0 for butanol, and 1.38 for 1-hexanol. Lines are only to aid visualization.

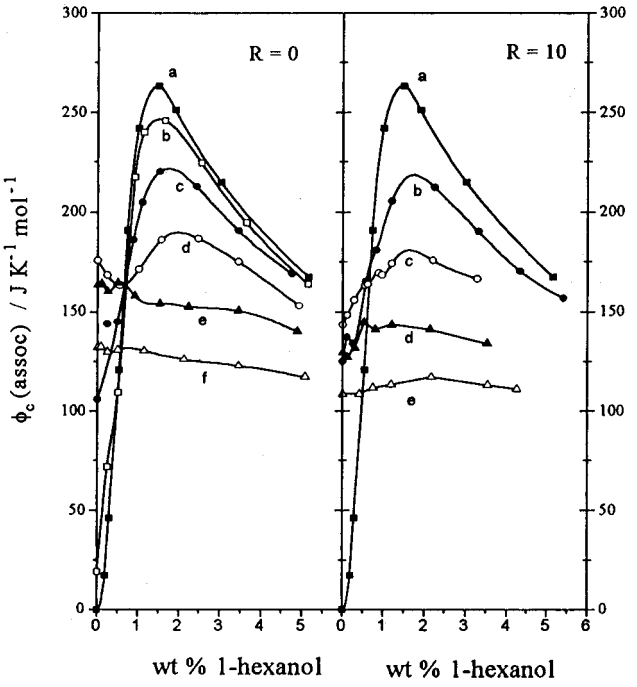


**Figure 5.** Associational part of the apparent molar heat capacity of 1-hexanol at 25 °C as a function of alcohol concentration for mixtures alcohol + ($p$ wt % AOT + $n$C$_{10}$) with $R = 0$ and 10. For $R = 0$, $p$ values are 0.0 (a), 0.48 (b), 2.02 (c), 5.05 (d), 10.25 (e), and 16.29 (f). For $R = 10$, $p$ values are 0.0 (a), 2.2 (b), 5.30 (c), 10.14 (d), and 15.05 (e). Data for $p = 0.0$, *i.e.*, for the binary 1-hexanol + $n$C$_{10}$, are from ref 15b. Lines are only to aid visualization.

for the other linear and branched alcohols there is a strong decrease of $\eta$ with alcohol concentration.

A hydrodynamic radius $r_h$ of the reverse micelles in the presence of alcohol can be estimated from the diffusion coefficients $D(\phi')$ in eq 10, using the Stokes−Einstein relation with the measured kinematic viscosities and densities of the medium. The results are shown in Figure 4; it can be seen that with increasing alcohol concentration $r_h$ increases for methanol and ethanol, remains practically constant for propanol, and decreases for butanol, hexanol, hexadecanol, and the branched alcohols. The changes on $r_h$ observed in Figure 4 are considerable since, for example, for methanol $r_h$ increases *ca.* 30% on going from zero alcohol concentration to 0.85 wt % and decreases *ca.* 60% for hexadecanol when the solution contains 1.78 wt % of the alcohol. A behavior as that seen in Figure 4 has been recently found[11] using DLS at very low alcohol concentrations (less than 0.5 wt %) for ethanol to nonanol in microemulsions ($R = 30$) formed by AOT + W + $n$C$_{10}$; in ref 11, however, $r_h$ for propanol was found to increase with alcohol concentration. For a given alcohol concentration, the behavior of $r_h$ with alcohol carbon number and with $R$ is also interesting. This behavior is shown in Figure 4 using the present data ($R = 10$) and that in ref 11 ($R = 30$) and ref 10 ($R = 20$). As a function of the alcohol carbon number, for each $R$ ratio, $r_h$ values are close for the shorter alcohols (methanol to propanol) and then decrease markedly on going to the longer ones, where $r_h$ is again practically constant or increases slightly. On the other hand, for any given alcohol at the same (or very close) concentration, $r_h$ increases with $R$. It appears then that, on going from a micellar domain ($R = 10$) to a microemulsion region ($R = 30$), the size of the reverse micelles increases, but their behavior with alcohol concentration or carbon number is qualitatively the same.

The swelling and shrinkage of the reversed micelles in the presence of short and long alcohols, respectively, together with the behavior of the kinematic viscosities strongly suggest that methanol and ethanol are trapped in the water pool of the reverse micelles, while the other linear and branched alcohols are dispersed in the surrounding solvent and probably also incorporated into the micellar shell. This is consistent with the solubility behavior of alcohols in water and in $n$C$_{10}$; that is methanol and ethanol are soluble in water and sparingly soluble in $n$C$_{10}$, while for the other alcohols the situation is the contrary. In fact, at a given AOT concentration, it is possible to solubilize more methanol when $R = 10$ than when $R = 0$, *i.e.*, when reverse micelles are present. The above conclusions from the DLS measurements are helpful in the analysis of the heat capacity data that follows.

*Alcohol Apparent Heat Capacities.* Despite the success of eq 9 of giving a clear physical picture of the behavior of the AOT−W asembly or micellar matter, when an alcohol is added, the use of eq 8 is more convenient. The choice α = alcohol in eq 8 is based on two main considerations; namely they enable us (i) to relate the present results with the situation in other systems, namely, self-association of alcohols in inert solvents[14,15,29,30] and self-association and complex formation in alcohol + proton acceptor + inert solvent mixtures,[13,16] and (ii) to reach one of the goals of the present work, *i.e.*, to study the interactions of alcohol−reverse micelles through the knowledge of the behavior of the alcohol in the micellar solution.

The association part of the apparent molar heat capacity $\phi_c$(assoc) for 1-hexanol as a function of alcohol concentration in the mixtures alcohol + ($p$ wt % AOT + $n$C$_{10}$) with $R = 0$ and 10 and several $p$ values are shown in Figure 5. These experimental $\phi_c$(assoc) were obtained using eqs 1 and 8. Note that the limiting $\phi_c$(assoc) values go through a maximum as a function of AOT concentration. For comparison, in Figure 5 the alcohol $\phi_c$(assoc) for 1-hexanol + $n$C$_{10}$ from ref 15b is also

shown. For this binary mixture, $\phi_c$(assoc) shows a maximum which is a reflection of the high degree of structure or organization, produced by the formation of multimers, that takes place at low 1-hexanol concentrations.[15b] In Figure 5, $\phi_c$(assoc) increases rapidly, corresponding to the formation of structure caused by the coming together of 1-hexanol molecules over long distances to form multimers; with further increase in concentration $\phi_c$(assoc) decreases because alcohol molecules must come together to form multimers over shorter distances; that is, the entropy decrease produced by the formation of a multimer is, at these concentrations, smaller than that occurring in the more dilute region. When AOT is added, either in free form ($R = 0$) or forming reverse micelles ($R = 10$), the alcohol $\phi_c$(assoc) is seen in Figure 5 to decrease markedly until for high $p$ values the maximum disappears. This behavior is identical to that found when a nonsurfactant proton acceptor is added to an alcohol−hydrocarbon mixture. In ref 13 $\phi_c$(assoc) was measured as a function of alcohol concentration for ternary solutions of the type 1-hexanol + (methyl acetate + *n*-dodecane); here, as the concentration of methyl acetate (MA) increased, the maximum in $\phi_c$(assoc) decreased and moved to higher 1-hexanol concentrations, *i.e.*, the same behavior seen in Figure 5. The decrease and displacement of $\phi_c$(assoc) was shown to be due to the formation of a 1:1 complex between MA and 1-hexanol, *i.e.*, to the formation of a H-bond between the carbonyl group in MA and the hydroxyl group in the 1-alcohol. The formation of this new species in solution competes with the formation of self-associated species, and as a result $\phi_c$(assoc) decreases. This competition can be "tuned" by changing the amount of proton acceptor used in the ternary mixture; the more proton acceptor molecules present, the larger the number of complexes formed and the more pronounced the $\phi_c$(assoc) drop. Hence, the behavior of $\phi_c$(assoc) for the present systems for both $R = 0$ and 10 must be attributed to the formation of a complex between 1-hexanol and AOT which acts as a proton acceptor. The scale used in Figure 5 to show $\phi_c$(assoc) at different AOT concentrations or $p$ values makes difficult the comparison between the $R = 0$ and 10 cases. Figure 6 shows $\phi_c$(assoc) using a wider scale for three $p$ values. It is seen that for $p = 2$ $\phi_c$(assoc) is independent of $R$; at this AOT concentration, few AOT molecules are available to interact with the alcohol to form a complex, and hence the self-association of 1-hexanol is the dominant effect. At higher $p$ values in Figure 6 $\phi_c$(assoc) is smaller when the system contains reverse micelles than when AOT molecules are freely dispersed in the hydrocarbon media. The further decrease of $\phi_c$(assoc) from the corresponding 1-hexanol + $n$C$_{10}$ curve for $R = 10$ indicates that when reverse micelles are present, either there are more 1-hexanol/AOT complexes formed or, alternatively, there are less complexes, but with a more severe decrease of the association entropy. The application of the TK model to the data in Figures 5 and 6, and to the corresponding data for all other alcohols used here, will enable us to distinguish between these two alternatives (see below).

The chemical structure of AOT indicates that the alcohol−AOT complex might be formed through a hydrogen bond between the hydroxyl group of the alcohol and the carbonyl group of AOT and/or via a strong hydroxyl−polar head interaction. In order to try to distinguish between these two possibilities, Figure 7 shows the measured $\phi_c$(assoc) for 1-hexanol + (5 wt % DOS + $n$C$_{10}$) and compare these data with that for 1-hexanol + $n$C$_{10}$ and for 1-hexanol + (5 wt % AOT + $n$C$_{10}$), *i.e.*, the $R = 0$ case. DOS is an interesting compound whose dielectric properties in cyclohexane have been carefully compared with those of AOT[31] and whose chemical structure

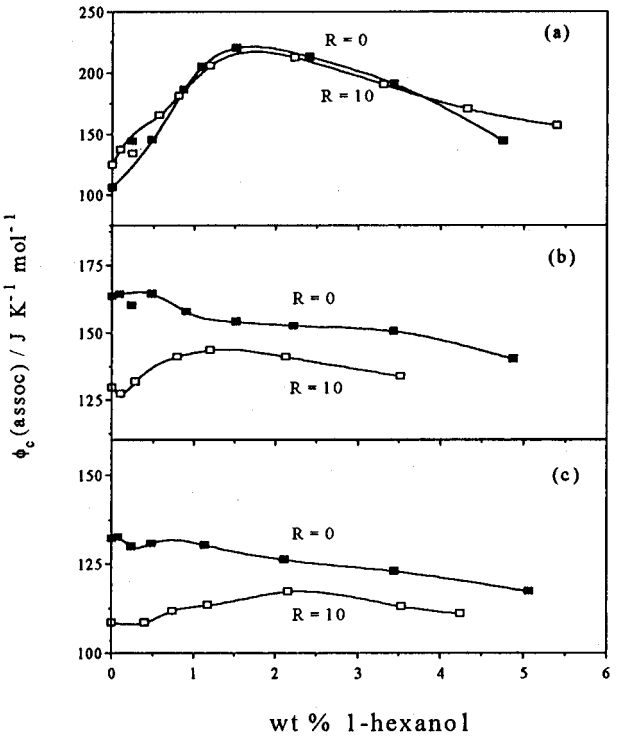


**Figure 6.** Associational part of the apparent molar heat capacity of 1-hexanol at 25 °C as a function of alcohol concentration for mixtures alcohol + ($p$ wt % AOT + $n$C$_{10}$) with $R = 0$ and 10. For $R = 0$, $p$ values are 2.02 (a), 10.25 (b), and 16.29 (c). For $R = 10$, $p$ values are 2.2 (a), 10.14 (b), and 15.05 (c). Lines are only to aid visualization.

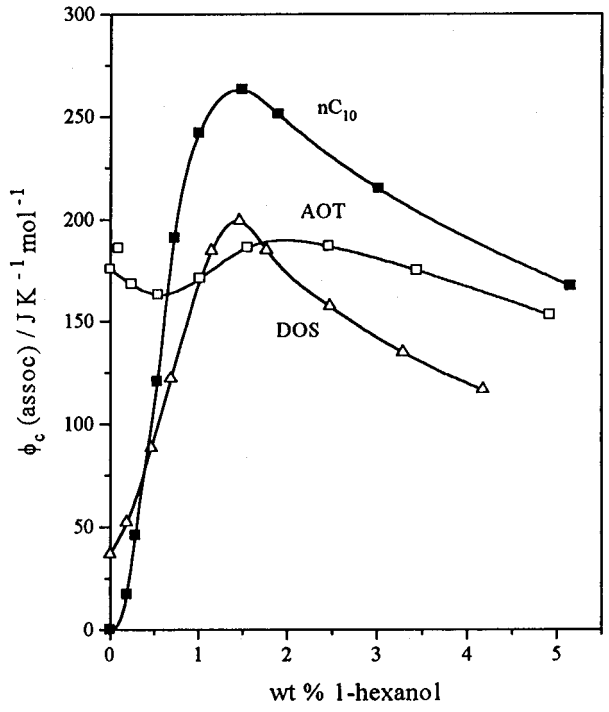


**Figure 7.** Associational part of the apparent molar heat capacity of 1-hexanol at 25 °C as a function of alcohol concentration for mixtures 1-hexanol + (5.05 wt % AOT + $n$C$_{10}$) (□), and 1-hexanol + (5.3 wt % DOS + $n$C$_{10}$) (△). For comparison $\phi_c$(assoc) data for the binary 1-hexanol + $n$C$_{10}$ (■) from ref 15b are also shown. DOS is dioctyl succinate. Lines are only to aid visualization.

is very similar to that of AOT, the difference being that DOS lacks the $SO_3Na$ group present in AOT. The comparison between the curves in Figure 7. indicates that DOS and AOT behave quite differently: while for AOT the $\phi_c$(assoc) maximum has almost disappeared, for DOS this maximum is preserved

**TABLE 1: Alcohol Limiting Apparent Molar Heat Capacities (in J $K^{-1}$ $mol^{-1}$) at 25 °C for Methanol and 1-Hexanol in Mixtures Alcohol + (*p* wt % AOT + $nC_{10}$) with $R = 0$ and 10**

| methanol $R = 0$ | | methanol $R = 10$ | |
|---|---|---|---|
| *p* | lim $\phi_c$(assoc) | *p* | lim $\phi_c$(assoc) |
| 1.05 | 137 ± 16 | 0.21 | 128 ± 37 |
| 2.03 | 176 ± 11 | 0.43 | 134 ± 27 |
| 2.54 | 201 ± 11 | 0.51 | 246 ± 20 |
| 3.04 | 191 ± 15 | 1.24 | 281 ± 16 |
| 3.04 | 190 ± 11 | 1.60 | 242 ± 10 |
| 3.60 | 257 ± 12 | 1.91 | 190 ± 11 |
| 3.77 | 206 ± 12 | 2.35 | 188 ± 19 |
| 5.00 | 214 ± 14 | 3.55 | 157 ± 10 |
| 6.22 | 179 ± 11 | 4.33 | 141 ± 10 |
| 7.50 | 144 ± 11 | 7.27 | 105 ± 12 |
| 10.28 | 144 ± 11 | 13.04 | 101 ± 12 |
| 13.25 | 142 ± 12 | | |
| 1-hexanol $R = 0$ | | 1-hexanol $R = 10$ | |
| *p* | lim $\phi_c$(assoc) | *p* | lim $\phi_c$(assoc) |
| 0.48 | 19 ± 20 | 2.16 | 106 ± 11 |
| 2.02 | 106 ± 16 | 2.20 | 125 ± 11 |
| 5.05 | 176 ± 13 | 3.01 | 133 ± 11 |
| 10.25 | 164 ± 10 | 3.79 | 152 ± 11 |
| 16.29 | 132 ± 10 | 5.30 | 144 ± 10 |
| | | 8.62 | 133 ± 11 |
| | | 10.14 | 130 ± 11 |
| | | 11.34 | 142 ± 10 |
| | | 15.05 | 109 ± 11 |

and its limiting $\phi_c$(assoc) is much smaller than in the AOT case. The decrease of $\phi_c$(assoc) from the 1-hexanol + $nC_{10}$ case to the DOS case is due to the formation of H-bonds between the hydroxyl group in 1-hexanol and the COO group in DOS, which acts as a proton acceptor. Hence, the difference between the AOT and DOS curves is due to the hydroxyl−$SO_3$ interaction, which is clearly dominant. It appears then that, in agreement with the findings in ref 9, the alcohol−AOT complex is most probably formed via the interaction of the hydroxyl group in the alcohol and the ionic head of AOT.

*Application of the TK Model.* In the TK model described above there are two parameters, $K_{11}^{\varphi}$ and $\Delta H_{11}^{\circ}$, characterizing the formation of a 1:1 alcohol−AOT complex. These two parameters can be obtained, in the cases of methanol and 1-hexanol, from a fit of eq 6 to the experimental lim $\phi_c$(assoc)-($x_1 \rightarrow 0$) data from eq 5 and reported in Table 1. In using eq 5, the lim $\phi_c$ were obtained through extrapolation to zero alcohol concentration, and the lim $\phi_c^b(x_1 \rightarrow 0)$ were from ref 15b. The results of the fitting are given in Table 3. Here, the necessary molar volumes and molar volume ratios employed by the TK model are given in Table 2. Figures 8 and 9 show for these two alcohols the experimental limiting $\phi_c$(assoc) values and the TK model curves. Clearly, the TK model is able to describe correctly the experimental behavior of the lim $\phi_c$(assoc)($x_1 \rightarrow 0$). The increase in the limiting $\phi_c$(assoc) with increasing AOT concentration corresponds to an increase in the probability that an alcohol molecule at infinite dilution should be complexed with AOT. With further increase of AOT, the limiting $\phi_c$(assoc) decreases, since the possibility of the complex being destroyed on raising the temperature is smaller. For both alcohols, the $K_{11}^{\varphi}$ value for $R = 0$ is bigger than for $R = 10$, implying that when reverse micelles are present there are less alcohol−AOT complexes in the mixture. These $K_{11}^{\varphi}$ values together with the corresponding $\Delta H_{11}^{\circ}$ values indicate a larger entropy decrease for the formation of alcohol−AOT complexes when $R = 10$, producing a smaller $\phi_c$(assoc) in Figure 6. The more negative

**TABLE 2: Molar Volumes of the Pure Alcohols (in $cm^3$ $mol^{-1}$) and Molar Volume Ratios Employed by the TK Model at 25 °C**

| alcohol | *V* | $r^a$ $R = 0$ | $r^b$ $R = 10$ | $r_1{}^c$ | $r_A{}^d$ |
|---|---|---|---|---|---|
| methanol | 40.74[e] | 9.75 | 1.29 | 4.81 | 1.00 |
| ethanol | 58.67[e] | 6.77 | 0.89 | 3.34 | 1.44 |
| 1-propanol | 75.16[f] | 5.29 | 0.70 | 2.61 | 1.85 |
| 1-butanol | 91.92[e] | 4.32 | 0.57 | 2.13 | 2.26 |
| 1-hexanol | 125.37[e] | 3.17 | 0.42 | 1.56 | 3.08 |
| 1-octanol | 158.51[f] | 2.51 | 0.33 | 1.24 | 3.89 |
| 1-dodecanol | 224.63[e] | 1.77 | 0.23 | 0.87 | 5.52 |
| 1-hexadecanol | 292.22[e] | 1.36 | 0.18 | 0.67 | 7.18 |
| 3-ethyl-3-pentanol | 138.41[g] | 2.87 | 0.38 | 1.42 | 3.40 |
| 2-methylcyclohexanol | 123.28[h] | 3.22 | 0.43 | 1.59 | 3.03 |
| cholesterol | 359.58[i] | 1.10 | 0.15 | 0.54 | 8.83 |

[a] $r = V_{AOT}/V_{alcohol}$ with $V_{AOT} = 397.32$ $cm^3$ $mol^{-1}$ from ref 37. [b] $r = V'_{AOT}/V_{alcohol}$ with $V'_{AOT} = x_{AOT}V_{AOT} + x_WV_W = 52.48$ $cm^3$ $mol^{-1}$. [c] $r_1 = V_{n-decane}/V_{alcohol}$ with $V_{n-decane} = 195.52$ $cm^3$ $mol^{-1}$ from ref 15b. [d] $r_A = V_{alcohol}/40.74$ and $r_B = V_{AOT}/40.74 = 9.75$ for $R = 0$ and $r_B = V'_{AOT}/40.74 = 1.29$ for $R = 10$. [e] From ref 15b. [f] From ref 38. [g] From ref 29. [h] From ref 30b (mixed isomers). [i] From ref 14.

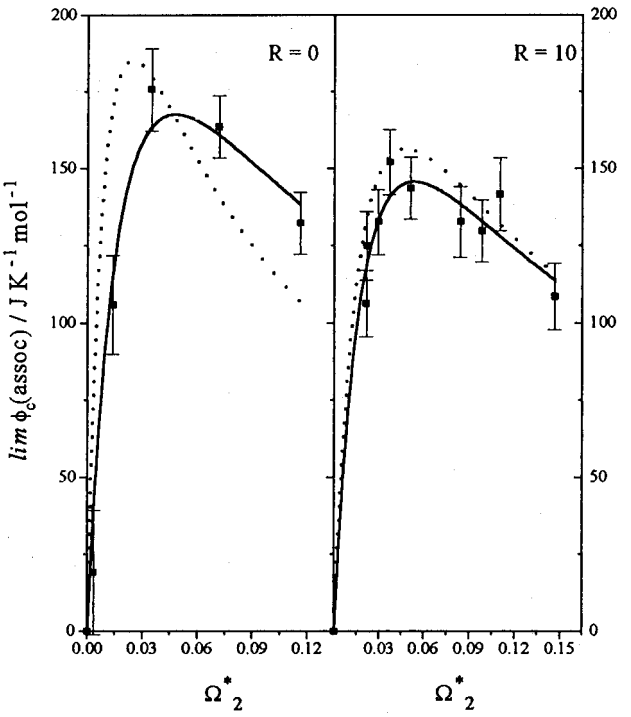


**Figure 8.** Experimental lim $\phi_c$(assoc)($x_1 \rightarrow 0$) at 25 °C (from Table 1) for 1-hexanol in the mixtures 1-hexanol + AOT + $nC_{10}$ with $R = 0$ and 10 against $\Omega_2^*$, the volume fraction of AOT in the AOT + $nC_{10}$ mixture ($R = 0$) and the volume fraction of AOT + W in the AOT + W + $nC_{10}$ mixture ($R = 10$). Solid lines are a fit to the experimental data using the TK model, namely, eq 6, producing the alcohol−AOT complex formation parameters given in the text. Dotted lines are calculated using eq 6 with the parameters given in Table 3.

entropy of complex formation for $R = 10$ might be due to the alcohol molecules penetrating the micellar shell to associate with the AOT molecules. The localization of the hydroxyl group of the alcohols in the micellar interface has also been used to interpret fluorescence intensity data of indoleacetate anions incorporated into AOT reverse micelles.[32]

The association part of the alcohol apparent molar heat capacities $\phi_c$(assoc) is given in the TK model by eq 2. The self-association volumetric equilibrium constants $K_i^{\varphi}$ ($i = 2-4$) and the enthalpy of the alcohol−alcohol hydrogen bond, $\Delta H^{\circ}$, were obtained previously[15b] using the TK model in studying the self-association of alcohols in inert solvents. In ref 15b, it was found that tetramers were by far the predominant

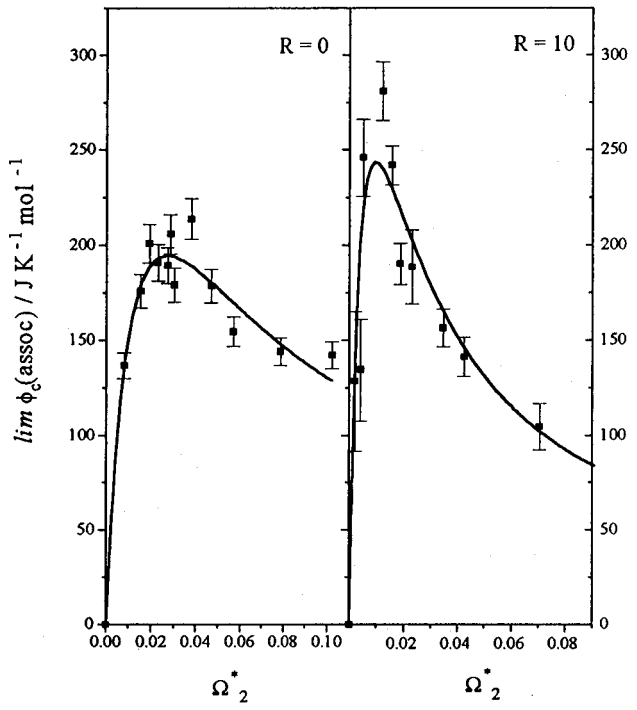


**Figure 9.** Experimental lim $\phi_c$(assoc)($x_1 \rightarrow 0$) at 25 °C (from Table 1) for methanol in the mixtures methanol + AOT + $n$C$_{10}$ with $R = 0$ and 10 against $\Omega_2^*$, the volume fraction of AOT in the AOT + $n$C$_{10}$ mixture ($R = 0$) and the volume fraction of AOT + W in the AOT + W + $n$C$_{10}$ mixture ($R = 10$). Solid lines are a fit to the experimental data using the TK model, namely, eq 6, producing the alcohol−AOT complex formation parameters given in the text.

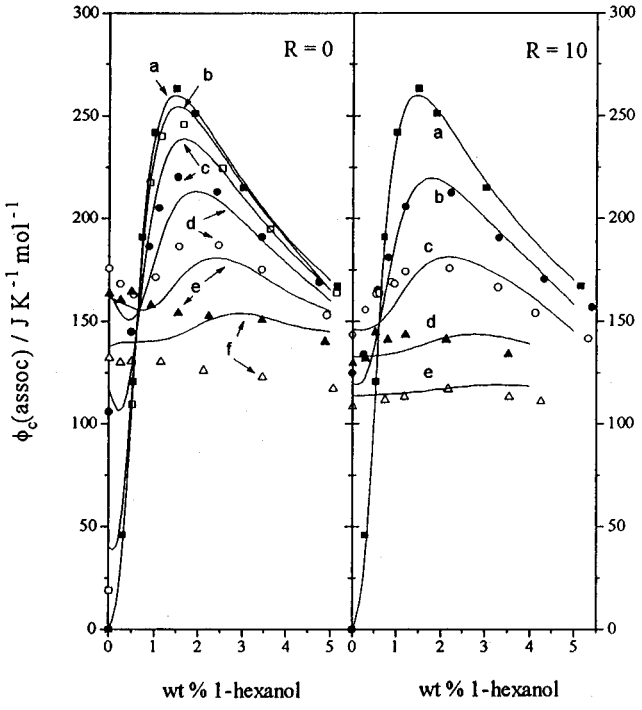


**Figure 10.** TK model predictions (continuous lines) for the associational part of the apparent molar heat capacity of 1-hexanol at 25 °C as a function of alcohol concentration for mixtures alcohol + ($p$ wt % AOT + $n$C$_{10}$) with $R = 0$ and 10. The predictions were done using eq 2 with the alcohol−AOT complex formation parameters fitted to only the limiting $\phi_c$(assoc) in Table 1 (values given in the text), and the self-association parameters from ref 15b. For $R = 0$, $p$ values are 0.0 (a), 0.48 (b), 2.02 (c), 5.05 (d), 10.25 (e), and 16.29 (f). For $R = 10$, $p$ values are 0.0 (a), 2.2 (b), 5.30 (c), 10.14 (d), and 15.05 (e). Data for $p = 0.0$, *i.e.*, for the binary 1-hexanol + $n$C$_{10}$ are from ref 15b.

species, and hence the use of only three $K_i^{\varphi}$ equilibrium constants is justified. Using the TK self-association parameters from ref 15b and the above reported values for $K_{11}^{\varphi}$ and $\Delta H_{11}^{\circ}$ for 1-hexanol, Figure 10 shows the predicted $\phi_c$(assoc) from eq 2 as a function of alcohol concentration for $R = 0$ and 10. The predictions are excellent, considering that for $p \neq 0$ the TK curves in Figure 10 were calculated using the complex formation parameters fitted to only the limiting $\phi_c$(assoc) values, and the self-association parameters fitted to the binary mixture 1-hexanol + inert solvent. It appears then that the TK model is able to describe properly the alcohol−AOT interactions, as seen by heat capacity measurements, in the presence or absence of reverse micelles. In agreement with experiment, at the same $p$ value in Figure 10 $\phi_c$(assoc) is predicted by the TK model to be smaller for $R = 10$ than for $R = 0$. For $R = 10$ and in the absence of alcohol, the AOT concentration in the media, *i.e.*, the AOT not forming part of any micelle, is equal to its cmc value; since this cmc is very low, when the alcohol is added the smaller $\phi_c$(assoc) for $R = 10$ in Figure 10b can only be explained if some AOT molecules are displaced from the micelle toward the bulk solution to complex with the alcohol.

The number of experiments that are necessary to produce a collection of points as those seen in Figures 8 and 9 is very large. In order to study more alcohols, as reported above, $\phi_c$(assoc) was obtained for a series of alcohols at a single $p$ value (5 wt %) and $R = 0$ and 10. Using eq 2, with the self-association parameters from refs 15b and 28, $K_{11}^{\varphi}$ and $\Delta H_{11}^{\circ}$ were fitted to the $\phi_c$(assoc) data as a function of alcohol concentration. The results are given in Table 4. In order to compare the two procedures to obtain the alcohol−AOT thermodynamic parameters, both were applied to the 1-hexanol case. With the parameters obtained from the $p = 5$ fitting (see Table 4), the limiting $\phi_c$(assoc) at any $p$ value were calculated using eq 6 and are shown in Figure 8. It can be seen that the two fittings are equivalent for both $R = 0$ and 10. Hence, the thermodynamic parameters characterizing the 1-alcohol and branched alcohol−AOT complexes are those displayed in Table 4.

**TABLE 3: Volumetric Equilibrium Constants and Enthalpies (in kJ mol$^{-1}$) at 25 °C for Methanol−AOT and 1-Hexanol−AOT Complex Formation**[a]

| alcohol | $K_{11}^{\varphi}$ $R = 0$ | $-\Delta H_{11}$ $R = 0$ | $K_{11}^{\varphi}$ $R = 10$ | $-\Delta H_{11}$ $R = 10$ |
|---|---|---|---|---|
| methanol | 473 ± 25 | 24.1 ± 0.3 | 261 ± 21 | 27.0 ± 0.5 |
| 1-hexanol | 90 ± 12 | 22.3 ± 0.5 | 27 ± 3 | 20.8 ± 0.3 |

[a] Obtained from a fit of eq 6 to the data in Table 1.

**TABLE 4: Volumetric Equilibrium Constants and Enthalpies (in kJ mol$^{-1}$) at 25 °C for Alcohol−AOT Complex Formation**[a]

| alcohol | $K_{11}^{\varphi}$ $R = 0$ | $-\Delta H_{11}$ $R = 0$ | $\sigma^b$ | $K_{11}^{\varphi}$ $R = 10$ | $-\Delta H_{11}$ $R = 10$ | $\sigma^b$ |
|---|---|---|---|---|---|---|
| methanol | 520 | 25.6 | 8.4 | 269 | 26.8 | 3.9 |
| ethanol | 474 | 23.9 | 47.7 | 251 | 31.8 | 12.9 |
| 1-propanol | 430 | 27.6 | 19.8 | 75 | 23.8 | 7.2 |
| 1-butanol | 280 | 26.4 | 17.6 | 71 | 23.7 | 6.2 |
| 1-hexanol | 175 | 23.4 | 6.1 | 30 | 21.5 | 7.0 |
| 1-octanol | | | | 24 | 20.7 | 6.4 |
| 1-dodecanol | 150 | 24.3 | 7.5 | 23 | 21.3 | 8.7 |
| 1-hexadecanol | 150 | 24.3 | 11.6 | 11 | 21.2 | 16.0 |
| 2-methylcyclohexanol[c] | 74 | 21.2 | 3.0 | 10 | 20.0 | 6.8 |
| 3-ethyl-3-pentanol | 23 | 22.4 | 5.4 | 5 | 21.9 | 3.4 |
| cholesterol | 42 | 24.7 | 17.8 | 4 | 18.8 | 30.6 |

[a] Obtained from a fit of eq 2 to $\phi_c$(assoc) data at $p = 5$. [b] Standard deviation of fit in J K$^{-1}$ mol$^{-1}$. [c] Mixed isomers.

*Heat Capacities of Transfer.* From the data in Table 1 or the TK curves in Figures 8 and 9, it is possible to obtain the

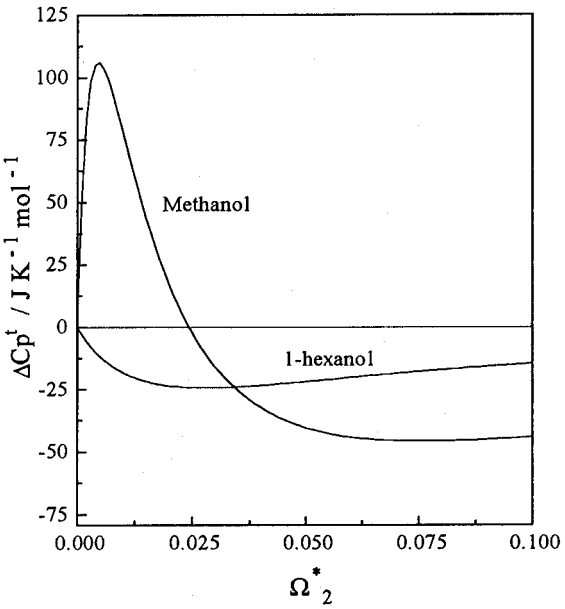


**Figure 11.** Heat capacity of transfer for methanol and 1-hexanol, at infinite dilution, against $\Omega_2^*$ at 25 °C. The transfer is from a mixture without AOT micelles ($R = 0$) to a mixture with reverse AOT micelles ($R = 10$). Curves were calculated using eqs 6 and 11 with the alcohol−AOT complex formation parameters given in the text.

so-called heat capacity of transfer $\Delta C_p^t$ as

$$\Delta C_p^t = \lim \phi_c(\text{assoc})(x_1 \rightarrow 0)[R{=}10] - \lim \phi_c(\text{assoc})(x_1 \rightarrow 0)[R{=}0] \quad (11)$$

which represents the change in heat capacity when an alcohol molecule, at infinite dilution, is transfered from a solution where AOT is freely dispersed in the inert solvent to a mixture containing reverse AOT micelles. On purely thermodynamic grounds,[33] the enthalpy of transfer $\Delta H^t$ is expected to be posisitve for an order-destroying process, *i.e.*, for a transfer that reduces structure in the system and increases its entropy; since order falls with increasing temperature at constant pressure $\Delta C_p^t = [\delta \Delta H^t/\delta T]_p$ must be negative for such a process. Using eqs 6 and 11 with the $K_{11}^{\varphi}$ and $\Delta H_{11}^{\circ}$ values given above, the $\Delta C_p^t$ for methanol and 1-hexanol as a function of AOT concentration can be calculated and are shown in Figure 11.

For 1-hexanol in Figure 11, $\Delta C_p^t < 0$ at all AOT concentrations, suggesting that this alcohol partially disorders the AOT micelles. As discussed above, this order-destroying process occurs through (i) the withdrawal of some AOT molecules from the micellar shell to form hexanol−AOT complexes in the surrounding inert media and (ii) the penetration of 1-hexanol to the micellar shell, with its hydroxyl group directed toward the water pool and with its hydrophobic tail parallel to those of AOT, allowing the alcohol−AOT complex to be formed. Both these mechanisms increase micelle curvature, promoting the formation of smaller micelles (but more since the water content is kept constant), rendering a smaller diffusion coefficient and hydrodynamic radius as obtained from the DLS results (Figure 4) and predicted from a molecular geometry point of view.[4,34] The above conclusions for 1-hexanol can be extended to butanol and longer alcohols. It appears then that for these alcohols the alcohol−AOT complex is formed both in the micelle and in the surrounding media, establishing an equilibria where alcohol molecules must be constantly interchanging between the two locations.

For methanol, $\Delta C_p^t > 0$ at low AOT concentration, implying that the introduction of this alcohol decreases the entropy of the system. This is consistent with the conclusion from the DLS results, namely, that methanol molecules place themselves in the micelle water pool. Additional evidence for this conclusion can be obtained considering the transfer of methanol, at infinite dilution, from the situation where it is surrounded by an inert solvent (equivalent to the $R = 0$ case at low AOT concentration) to the situation where it is surrounded by water molecules (equivalent to the $R = 10$ case). Using the data in refs 15b and 35, this $\Delta C_p^t = 156 - 72 = 84$ J K$^{-1}$ mol$^{-1}$; clearly, the sign and magnitude (see Figure 11) of this $\Delta C_p^t$ support the conclusion that at $R = 10$ the added methanol is located in the water pool. In Figure 11, for methanol at higher AOT concentrations $\Delta C_p^t < 0$; that is, in this concentration region, methanol has a disordering effect in the micelle. This can be understood considering the transfer of methanol, at infinite dilution, from the situation where it is surrounded by an inert solvent to the situation where it is surrounded by proton acceptor molecules such as methyl acetate which have the same COO group as AOT. From the data in refs 15b and 16, this $\Delta C_p^t = 16 - 72 = -56$ J K$^{-1}$ mol$^{-1}$, in agreement with the sign and magnitude seen in Figure 11. This result suggests that at high AOT concentrations methanol molecules in the water pool complex with the AOT molecules in the micellar shell. The probability of a methanol molecule being at the border of the water pool increases as the micelle size decreases, and according to Figure 11, this size reduction must occur as the concentration of AOT increases (for $\Omega_2^* > 0.025$). This decrease has in fact been experimentally reported in ref 7 at $R = 30$ and corroborated by our own DLS experiments (not reported here). That the micelle size decreases as the concentration of AOT increases is, however, a controversial issue since other authors[36] have found that droplet size, in cyclohexane, toluene, and chlorobenzene at several fixed $R$ values ($R \leq 10$), is independent of AOT concentration. The overall results in Figure 11 for methanol indicate that the $K_{11}^{\varphi}$ and $\Delta H_{11}^{\circ}$ values for this alcohol (and for ethanol) at $R = 10$ in Table 4 are only truly meaningful at $\Omega_2^* > 0.025$ since at lower AOT concentrations these two alcohols are interacting mainly with water. In this context, propanol appears to be a limiting case between the behavior of methanol and ethanol and that for butanol and longer alcohols.

*Fundamental Equilibrium Constants.* The volumetric equilibrium constants $K_{11}^{\varphi}$ in Table 4 for the different alcohols interacting with AOT depend on the size of the molecules involved. This dependence is shown in Figure 12a for $R = 0$ and 10. A similar dependence was found previously[9] using IR spectroscopy and carbon tetrachloride as solvent. These volumetric equilibrium constants can be transformed into a unique more fundamental or intrinsic equilibrium constant $K_{11}$, which is independent of molecular size and describes the association between the hydroxyl group in the alcohol and the ionic head of the AOT molecule. This can be achieved[15b,16] using the Flory lattice theory giving

$$K_{11}^{\varphi} = K_{11}(r_A^{-1} + r_B^{-1})\frac{\sigma_A \sigma_B}{\sigma_{AB}}\left(\frac{\omega^2}{z}\right) \quad (12)$$

where $r_A$ and $r_B$ are the number of segments in the alcohol and the proton acceptor molecules, respectively, given in Table 2 and defined by dividing the molar volumes by the molar segmental volume, which, as in refs 15b and 16, is taken as the molar volume of methanol (40.7 cm$^3$ mol$^{-1}$). In eq 12, $\omega$ is the flexibility parameter for the complex and $z$ is the lattice coordination number, taken as in ref 15b to be 1.69 and 10; $\sigma_A$ and $\sigma_B$ are symmetry numbers for the alcohol and AOT

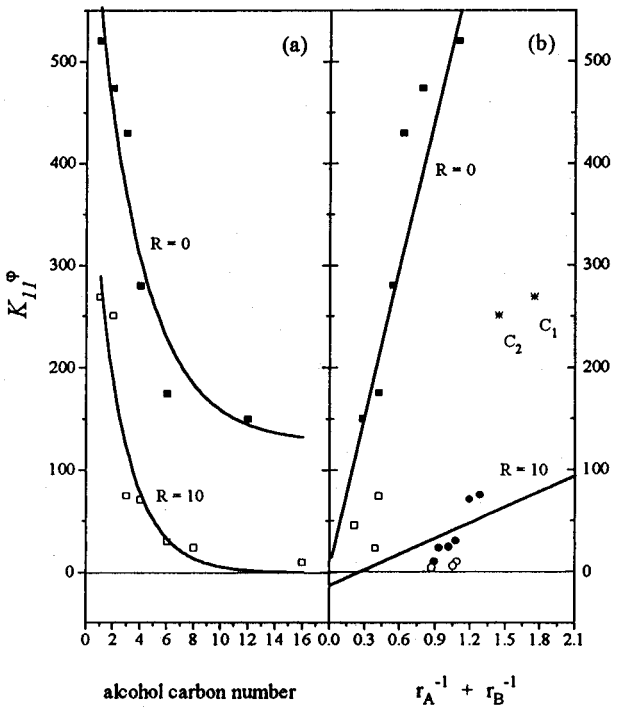


**Figure 12.** Volumetric equilibrium constants against alcohol carbon number (a) and against $r_A^{-1} + r_B^{-1}$ (b) at $R = 0$ and 10. In a, curves are only to aid visualization. In b, the straight lines are a fit to the $K_{11}^{\varphi}$ data according to eq 12, $C_1$ and $C_2$ denote methanol and ethanol, respectively, and the open symbols correspond to the three branched alcohols.

molecules taken equal to 2, but $\sigma_{AB} = 1$, reflecting the asymmetry of the complex. Equation 12 then translates the intermolecular $K_{11}^{\varphi}$ into the intergroup equilibrium constant $K_{11}$, through the molecular chain lengths $r_A$ and $r_B$, reflecting the entropy lowering involved in localizing the hydroxyl group (OH) in the alcohol and the ionic head groups in AOT, to form an OH−$SO_3$ interaction. Equation 12 is tested in Figure 12b through a plot of the $K_{11}^{\varphi}$ values in Table 4 against ($r_A^{-1} + r_B^{-1}$) from the data in Table 2. Reasonable agreement is indicated by the straight lines (only 1−alcohols taken) with slopes given by $K_{11}(\sigma_A\sigma_B\omega^2/\sigma_{AB}z) = 510$ for $R = 0$ and 51 for $R = 10$. Figure 12b shows that in the absence or presence of reverse micelles the 1-alcohol/AOT complex has different thermodynamic parameters; each of these two sets of parameters are independent of the alcohol (and AOT) molecular size. For $R = 10$, methanol and ethanol clearly do not follow the same behavior shown by the rest of the linear alcohols; this is due to these alcohols being trapped in the micelle water pool as the light scattering results suggested. Using the above values for the slopes in Figure 12b and the several parameters in the Flory lattice theory together with an average value for the enthalpy of complex formation from Table 4 (methanol and ethanol excluded for $R = 10$), the thermodynamic parameters characterizing the linear alcohol−AOT complex are for $R = 0$

$$K_{11} = 446 \pm 45 \qquad \Delta H_{11}^{\circ} = -25.1 \pm 0.4 \text{ kJ mol}^{-1}$$

$$\Delta G_{11}^{\circ} = -15.1 \pm 0.3 \text{ kJ mol}^{-1}$$

$$\Delta S_{11}^{\circ} = -33.5 \pm 1.3 \text{ J K}^{-1} \text{ mol}^{-1} \quad (13)$$

and for $R = 10$ (for propanol and longer 1-alcohols)

$$K_{11} = 45 \pm 5 \qquad \Delta H_{11}^{\circ} = -22.0 \pm 0.3 \text{ kJ mol}^{-1}$$

$$\Delta G_{11}^{\circ} = -9.43 \pm 0.3 \text{ kJ mol}^{-1}$$

$$\Delta S_{11}^{\circ} = -42.1 \pm 1.0 \text{ J K}^{-1} \text{ mol}^{-1} \quad (14)$$

The values in eqs 13 and 14 must be taken as tentative, since in applying the TK model to the experimental data only a 1:1 complex has been considered, while, in principle, more than one alcohol molecule might be complexed with a given AOT molecule that possesses two COO groups and an ionic head. From the $\Delta G_{11}^{\circ}$ (or $K_{11}$) values in eqs 13 and 14, it is clear that the formation of alcohol−AOT complexes is less favorable in the presence of micelles. The results in eqs 13 and 14 for $\Delta H_{11}^{\circ}$ and $\Delta S_{11}^{\circ}$ can be understood in the following way: (i) the $\Delta H_{11}^{\circ}$ value indicates that the alcohol−AOT interaction is weaker when AOT is forming micelles ($|\Delta H_{11}^{\circ}|_{R=10} < |\Delta H_{11}^{\circ}|_{R=0}$) as a consequence of the fact that in the micellar shell the relative position of the alcohol and AOT molecules (their hydrocarbon tails parallel) is unfavorable for complexing as compared to the situation where both molecules are free in solution, and (ii) the entropic cost of forming an alcohol−AOT complex is much larger when micelles are present ($|\Delta S_{11}^{\circ}|_{R=10} > |\Delta S_{11}^{\circ}|_{R=0}$), reflecting the geometrical or steric difficulty for the penetration of the alcohol molecule to the micellar shell as compared with the alcohol-free AOT situation. Finally, note that in Figure 12 the $K_{11}$ values for the three branched alcohols are smaller than for the 1-alcohols, and in fact, for $R = 10$ there are very few branched alcohol−AOT complexes formed. This is a consequence of the molecular shape of these molecules, which translates into a steric hindrance over the hydroxyl group[29] and makes the complexation with AOT difficult.

**Acknowledgment.** This work was supported by the CONACYT (Grants 3904 and 0134) and by DAGAPA (Grant IN100595). We thank Reiji Tanaka of Osaka City University, Japan, for his generous gift of a DOS sample. In the early stages of this work, Donald Patterson of McGill University, Canada, contributed significantly, with his interest, his always relevant comments, and hospitality to one of us (S.P.C.). We also thank I. Espinosa and C. Garza for their technical assistance in the DLS experiments, and J. Kizling and M. Svensson for their comments on the manuscript.

**Supporting Information Available:** Heat capacity, kinematic viscosity, and diffusion coefficients data (10 pages). Ordering information is given on any current masthead page.

## References and Notes

(1) Langevin, D. In Reverse Micelles; Luisi, P. L., Straub, B. E., Eds.; Plenum Press: New York, 1984.
(2) Fendler, J. H. *Chem. Rev.* **1987**, *87*, 877.
(3) Langevin, D. *Phys. Scr.* **1986**, *T13*, 252.
(4) Pileni, M. P. *J. Phys. Chem.* **1993**, *97*, 6961.
(5) (a) Zulauf, M.; Eicke, J. F. *J. Phys. Chem.* **1979**, *83*, 480. (b) Dozier, W.; Kim, M. W.; Klein, J. *J. Chem. Phys.* **1987**, *87*, 1455.
(6) (a) Kotlarchyk, M.; Huang, J. S.; Chen, S. H. *J. Phys. Chem.* **1985**, *89*, 4882. (b) Robinson, B. H.; Toprakcioglu, C.; Dore, J. C.; Chieux, P. *J. Chem. Soc., Faraday Trans. 1* **1984**, *80*, 13. (c) Toprakcioglu, C.; Dore, J. C.; Robinson, H.; Howe, A.; Chieux, P. *J. Chem. Soc., Faraday Trans. 1* **1984**, *80*, 413.
(7) Assih, T.; Larché, F.; Delord, J. *J. Colloid Interface Sci.* **1982**, *89*, 35.
(8) (a) Tanaka, R.; Adachi, M. *Netsu Sokutei* **1991**, *18*, 138. (b) Morel, J. P.; Morel-Desrosiers, N. *J. Chim. Phys.* **1984**, *81*, 109.
(9) Ménassa, P.; Sandorfy, C. *Can. J. Chem.* **1985**, *63*, 3367.
(10) Howe, A. M.; Toprakcioglu, C.; Dore, J. C.; Robinson, B. H. *J. Chem. Soc., Faraday Trans. 1* **1986**, *82*, 2411.
(11) Lin, T. L.; Hu, Y.; Lee, T. T. *Prog. Colloid Polym. Sci.*, in press.

(12) Costas, M.; Patterson, D. *Thermochim. Acta* **1987**, *120*, 161.
(13) Costas, M.; Yao, Z.; Patterson, D. *J. Chem. Soc., Faraday Trans. 1* **1989**, *85*, 2211.
(14) Costas, M.; Patterson, D. *J. Chem. Soc., Faraday Trans. 1* **1985**, *81*, 655.
(15) (a) Costas, M.; Patterson, D. *J. Chem. Soc., Faraday Trans. 1* **1985**, 635. (b) Andreoli-Ball, L.; Patterson, D.; Costas, M.; Caceres-Alonso, M. *J. Chem. Soc., Faraday Trans. 1* **1988**, *84*, 3991.
(16) Deshpande, D. D.; Patterson, D.; Andreoli-Ball, L.; Costas, M.; Trejo, L. M. *J. Chem. Soc., Faraday Trans.* **1991**, *87*, 1133.
(17) Kehiaian, H.; Treszczanowicz, A. J. *Bull. Acad. Chim. Fr.* **1969**, *5*, 1561.
(18) Conte, S. D.; de Boor, C. *Elementary Numerical Analysis*, 2nd ed.; McGraw Hill: New York, 1972.
(19) Delord, P.; Larche, F. C. *J. Colloid Interface Sci.* **1984**, *98*, 277.
(20) Larche, F. C.; Delord, P. *Fluid Phase Equilib.* **1985**, *20*, 257.
(21) (a) Picker, P.; Leduc, A.; Philippe, P. R.; Desnoyers, J. E. *J. Chem. Thermodyn.* **1971**, *3*, 631. (b) Fortier, J. L.; Benson, G. C. *J. Chem. Thermodyn.* **1976**, *8*, 411.
(22) *CDATA*, Database of Thermodynamic and Transport Properties for Chemistry and Engineering. Department of Physical Chemistry, Prague Institute of Chemical Technology, **1991**. Distributed by FIZ Chemie GmbH, Berlin.
(23) Berne, B. J.; Pecora, R. *Dynamic Light Scattering*; John Wiley: New York 1976.
(24) Koppel, D. E. *J. Chem. Phys.* **1972**, *57*, 4814.
(25) (a) Eicke, H. F.; Rehak, J. *Helv. Chim. Acta* **1976**, *59*, 2883. (b) Eicke, H. F.; Kvita, P. In *Reverse Micelles*; Luisi, P. L., Straub, B. E., Ed.; Plenum Press: New York, 1984.
(26) Tanaka, R.; Okazaki, K.; Tsuzuki, H. *Chem. Lett.* **1995**, 1131.
(27) Desnoyers, J.; Perron, G. In *Surfactant Solutions. New Methods of Investigation*; Zana, R., Ed.; Marcel Dekker: New York, 1987; Vol. 22.
(28) Goto, A.; Yoshioka, H.; Manabe, M.; Goto, R. *Langmuir* **1995**, *11*, 4873.
(29) Caceres-Alonso, M.; Costas, M.; Andreoli-Ball, L.; Patterson, D. *Can. J. Chem.* **1988**, *66*, 989.
(30) (a) Perez-Casas, S.; Trejo, L. M.; Costas, M. *J. Chem. Soc., Faraday Trans.* **1991**, *87*, 1733. (b) Trejo, L. M.; Perez-Casas, S.; Costas, M.; Patterson, D. *J. Chem. Soc., Faraday Trans.* **1991**, *87*, 1739. (c) Perez-Casas, S.; Moreno-Esparza, R.; Costas, M.; Patterson, D. *J. Chem. Soc., Faraday Trans.* **1991**, *87*, 1745.
(31) Tanaka, R.; Tsuzuki, H.; Okazaki, K.; Kinoshita, T. *Fluid Phase Equilib.* **1996**, *123*, 131.
(32) Lissi, E. A.; Engel, D. *Langmuir* **1992**, *8*, 452.
(33) Kronberg, B.; Patterson, D. *J. Chem. Soc., Faraday Trans. 1* **1981**, *77*, 1223.
(34) Israelachvili, J. N.; Mitchell, D. J.; Ninham, B. W. *J. Chem. Soc., Faraday Trans. 2* **1976**, *72*, 1525.
(35) Benson, G. C.; D'Arcy, P. J.; Kiyohara, O. *J. Solution Chem.* **1980**, *9*, 931.
(36) Day, R. A.; Robinson, B. H. *J. Chem. Soc., Faraday Trans. 1* **1979**, *75*, 132.
(37) Caryl, C. R. *Ind. Eng. Chem.* **1941**, *33*, 731.
(38) Riddick, J. A.; Bunger, W. B.; Sakano, T. K. *Organic Solvents*, 4th ed.; Physical Properties and Methods of Purification. Techniques of Chemistry Volume II; Wiley Interscience: New York, 1986.